Chem

CellPress

Article

Photoinduced Skeletal Rearrangements Reveal Radical-Mediated Synthesis of Terpenoids

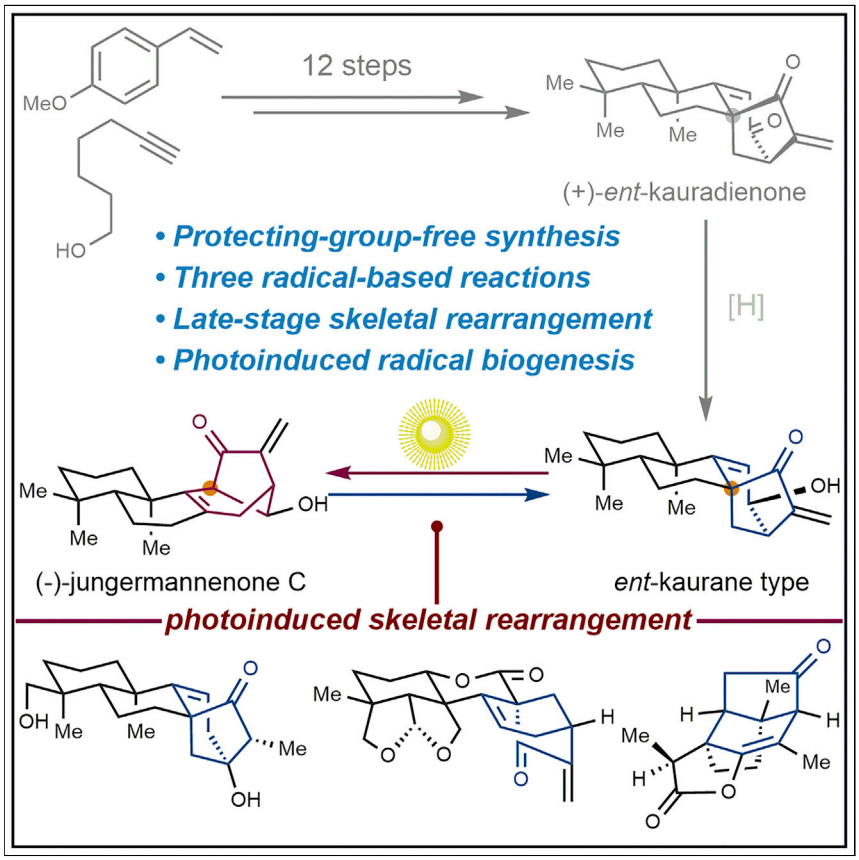

Protecting-group-free synthesis of (+)-*ent*-kauradienone and (−)-jungermannenone C has been accomplished through sequential applications of three radical-based reactions, including late-stage photoinduced skeletal rearrangements of bicyclo[3.2.1]octene ring systems. Further investigations on various terpenoids showed good functional-group tolerance and suggest that some terpenoids could also be produced via such photoinduced rearrangements pathways in nature. Our work demonstrates how paying more attention to unconventional radical mechanisms can reveal new chemistries that facilitate the synthesis of complex natural products.

Benke Hong, Weilong Liu, Jin Wang, ..., Zhi-Xiang Yu, Houhua Li, Xiaoguang Lei

lihouhua@hsc.pku.edu.cn (H.L.)
xglei@pku.edu.cn (X.L.)

HIGHLIGHTS

Protecting-group-free synthesis of *Isodon* diterpenoids

Photoinduced skeletal rearrangement of bicyclo[3.2.1] octenes

Late-stage photoinduced skeletal rearrangements of structurally diverse terpenoids

Hong et al., Chem *5*, 1–11
June 13, 2019
https://doi.org/10.1016/j.chempr.2019.04.023

Please cite this article in press as: Hong et al., Photoinduced Skeletal Rearrangements Reveal Radical-Mediated Synthesis of Terpenoids, Chem (2019), https://doi.org/10.1016/j.chempr.2019.04.023

Chem

CellPress

Article

Photoinduced Skeletal Rearrangements Reveal Radical-Mediated Synthesis of Terpenoids

Benke Hong,[1,2,6] Weilong Liu,[1,2,6] Jin Wang,[1,2,6] Jinbao Wu,[1,2] Yuichiro Kadonaga,[1,2] Pei-Jun Cai,[1] Hong-Xiang Lou,[4] Zhi-Xiang Yu,[1] Houhua Li,[5,*] and Xiaoguang Lei[1,2,3,7,*]

SUMMARY

Herein, we describe the protecting-group-free total synthesis of two structurally diverse *Isodon* diterpenoids, (+)-*ent*-kauradienone (3) and (−)-jungermannenone C (4), in 12 and 14 steps respectively, through sequential applications of three radical-based reactions, including the photoinduced skeletal rearrangements of bicyclo[3.2.1]octene ring systems. Further investigations of this photochemical radical rearrangement on a series of diverse terpenoids demonstrated both the unparalleled functional-group tolerance and the broad applicability of such late-stage photochemical rearrangements for the synthesis of structurally diverse and complex small molecules. Overall, the mild nature of late-stage photoinduced skeletal rearrangements might suggest that they are possible in a biological setting in unappreciated complimentary biosynthetic pathways.

INTRODUCTION

Deciphering the key chemical transformations of natural-product biosynthesis is of perennial importance in the fields of both natural-product chemistry and chemical biology.[1,2] For example, much inspired by the well-known "cyclization/late-stage P450-mediated oxidation" biosynthetic processes, total syntheses of a series of anticancer diterpenoids have been accomplished in recent years.[3–6] Biosynthetically, diterpenoids are derived from a common biosynthetic precursor, geranylgeranyl diphosphate (GGPP, 1), and are generated upon multistep carbocationic cyclization rearrangements catalyzed by terpenoid cyclases (Figure 1A).[7] Accordingly, extensive enzymatic and biomimetic studies have been reported in the literature.[8–12] We are interested in the biosynthetic pathways of complex diterpenoids and are especially keen on unconventional reaction mechanisms in which carbocations might not be involved.[13,14] Indeed, during our synthesis of *Isodon* diterpenoids, we identified a skeletal rearrangement of diterpenoids that proceed via a late-stage photochemical radical rearrangement of the bicyclo[3.2.1]octene ring system. To the best of our knowledge, this is the first time that a photoinduced skeletal rearrangement has been observed,[15,16] and it sheds light on a previously unknown and complimentary diterpenoid natural product biosynthesis pathway.[14]

RESULTS AND DISCUSSION

Skeletal Rearrangement of Bicyclo[3.2.1]octenes

Isodon diterpenoids are a unique family of polycyclic natural products, and more than 1,000 members have been isolated to date (Figure 1B).[17,18] It is widely accepted that these diverse diterpenoids—each with unique bioactivity—are biosynthetically derived from a common intermediate *ent*-pimarenyl cation (2) upon a series of

The Bigger Picture

The efficient synthesis of terpenoids is often complicated by their highly functionalized structures. Accordingly, deep insights gained in studies of terpenoid biosynthesis have deciphered chemical transformation mechanisms that synthetic chemists now widely exploit to construct the molecular architectures of terpenoids; however, there could be alternative biosynthetic pathways of terpenoids yet to be discovered. Herein, en route to complex *Isodon* diterpenoids, we discovered and subsequently harnessed a late-stage photoinduced skeletal rearrangement to successfully construct distinct bicyclo[3.2.1] octene ring systems. Further investigations on various terpenoids showed good functional-group tolerance and suggest that some terpenoids could also be produced via such photoinduced rearrangement pathways in nature. Our work demonstrates how paying more attention to unconventional radical mechanisms can reveal new chemistries that facilitate the synthesis of complex natural products.

Please cite this article in press as: Hong et al., Photoinduced Skeletal Rearrangements Reveal Radical-Mediated Synthesis of Terpenoids, Chem (2019), https://doi.org/10.1016/j.chempr.2019.04.023

enzymatic cyclizations starting from **1**. Subsequent successive carbocationic cyclization rearrangements generate the three known types of *Isodon* diterpenoid skeletons (**3**–**5**), each of which features a distinct bicyclo[3.2.1]octene ring system.[19,20] Of note, enzymatic carbocationic rearrangements have been proposed as being responsible for skeletal rearrangements among these *Isodon* diterpenoid types (Figure 1C): according to the initial biosynthetic hypothesis,[21,22] two possible carbocationic rearrangement pathways have been speculated for the skeletal rearrangement of *ent*-kaurane diterpenoids into jungermannenone diterpenoids. Such carbocationic rearrangements have long provided great inspiration for synthetic endeavors.[23–31] As exemplified in Figure 1C, and using acid-catalyzed carbocationic rearrangements, Hanson and co-workers and later Baran and co-workers reported the biomimetic skeletal rearrangements of *ent*-kaurane diterpenoids stevioside (**6a**) and steviol (**6b**), respectively, into *ent*-beyerane diterpenoid isosteviol (**5**).[29–31]

Much inspired by the aforementioned biosynthetic hypothesis, as well as biomimetic skeletal rearrangements reported by Hanson and co-workers and Baran and co-workers, we undertook a model study of the rearrangement of *ent*-kaurane-type skeletons into jungermannenone skeletons (Figure 2A). Starting from **7** (Tables S12 and S13; Figures S5 and S6) which was prepared in two steps from piperitone,[32] a series of acidic,[29–31] thermal,[33,34] radical,[35,36] and transition-metal-catalyzed[37] reaction conditions were tested, yet no rearrangement of the bicyclo[3.2.1]octene skeleton was observed (Table S1; Figures S25–S31). To our delight, upon 302 nm UV irradiation at room temperature (Table S2), **7** was transformed into **8** (Figures S32–S37) in 33% isolated yield; moreover, the transformation of **7** to **8** appeared as an equilibrium. Indeed, when **8** was subjected back to the same reaction conditions (Table S3), 52% of **7** was isolated. In both cases, the product compositions did not change upon longer exposure to UV irradiation—the products merely decomposed. The observed photoinduced skeletal rearrangement most likely proceeded via photochemical 1,3-acyl migration of the β,γ-unsaturated ketone (Figure 2B).[38,39] Detailed mechanistic studies conducted previously by Givens et al.,[40,41] Schaffner and co-workers,[42] and Robb and co-workers[43] suggested two plausible mechanisms that could explain such reactivity: a stepwise pathway that proceeds via a dissociation-recombination mechanism involving a cage radical pair **9** or a quasi-concerted pathway involving a bi-radical "tight" intermediate **10**.[44]

Radical processes are certainly not rare in natural-product biosynthesis, e.g., in the biosynthesis of ε-viniferin from resveratrol via a radical intermediate promoted by metalloenzymes[45,46] or the biosynthetic enantiodivergence of pyrrole-imidazole alkaloids.[47,48] Recently, an elegant total synthesis of ophiobolin sesterterpene via a reductive radical cascade cyclization was reported by Maimone and co-workers.[49,50] Trauner and co-workers also successfully achieved the biomimetic synthesis of furanocembranoid intricarene by using UV irradiation conditions.[51,52] However, no reports have proposed that the biosynthesis of *Isodon* diterpenoids proceeds via photochemical or radical rearrangement.[17,18] We envisaged that the late-stage assembly of bicyclo[3.2.1]octene skeletons could be accomplished efficiently by photoinduced skeletal rearrangement (Figure 2C). Accordingly, and given that photoinduced transformations can occur in mild conditions, there could be an alternative biogenesis route to *Isodon* diterpenoids wherein a spontaneous biosynthetic interconversion occurs between jungermannenones and *ent*-kauranes via skeletal rearrangements of bicyclo[3.2.1]octene under sunlight. To investigate this hypothesis, we shifted our focus onto the total synthesis of complex *Isodon* diterpenoids (*ent*-kaurane-type **3** and jungermannenone-type **4**).[21] As shown in Figure 2C, the distinct bicyclo[3.2.1]octene ring system of **4** could be derived from **3** by

[1]Beijing National Laboratory for Molecular Sciences, Key Laboratory of Bioorganic Chemistry and Molecular Engineering of Ministry of Education, College of Chemistry and Molecular Engineering, Peking University, Beijing 100871, China

[2]Department of Chemical Biology, Synthetic and Functional Biomolecules Center, Peking University, Beijing 100871, China

[3]Peking-Tsinghua Center for Life Sciences, Peking University, Beijing 100871, China

[4]Department of Natural Products Chemistry, MOE Key Lab of Chemical Biology, School of Pharmaceutical Sciences, Shandong University, Jinan 250012, China

[5]State Key Laboratory of Natural and Biomimetic Drugs, School of Pharmaceutical Sciences, Peking University, Beijing 100191, China

[6]These authors contributed equally

[7]Lead Contact

*Correspondence: lihouhua@hsc.pku.edu.cn (H.L.), xglei@pku.edu.cn (X.L.)

https://doi.org/10.1016/j.chempr.2019.04.023

Please cite this article in press as: Hong et al., Photoinduced Skeletal Rearrangements Reveal Radical-Mediated Synthesis of Terpenoids, Chem (2019), https://doi.org/10.1016/j.chempr.2019.04.023

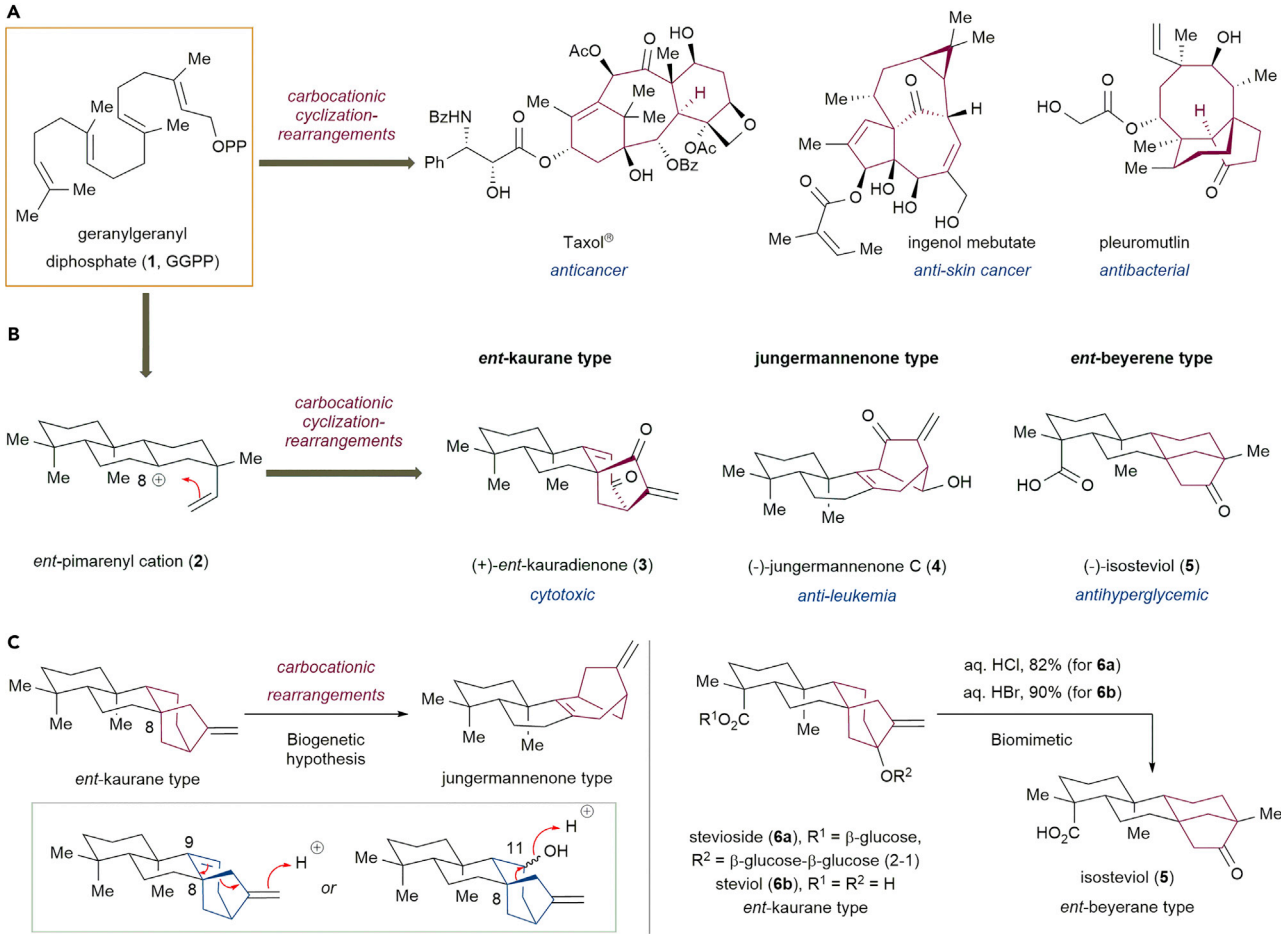

Figure 1. Structure, Biosynthesis, and Skeletal Rearrangement of Diterpenoids

(A) Selected complex diterpenoids with diverse biological activities.

(B) Proposed pathways employing carbocationic cyclization rearrangements for the biosynthesis of *Isodon* diterpenoids.

(C) Biosynthetic and biomimetic carbocationic rearrangements of *Isodon* diterpenoids.

photoinduced skeletal rearrangement. Whereas reductive radical cyclization is responsible for the direct assembly of the bicyclo[3.2.1]octene framework of **3**, *trans*-decalin **11** can be derived from aldehyde **12** through organo-SOMO catalysis.[53] The latter could be rapidly generated by coupling of commercially available alkyne **13** with styrene **14**.

Protecting-Group-free Synthesis of *Isodon* Diterpenoids 3 and 4

Our synthesis commenced with commercially available 6-heptyn-1-ol **13** (Figure 3); aldehyde **12** (Figures S40 and S41) was synthesized over three steps through sequential carboalumination and iodination[54] (**13** to **15**) and *B*-alkyl Suzuki-Miyaura coupling[55] (**15** to **16**, Figures S38 and S39) followed by Swern oxidation (**16** to **12**). Enantioselective radical cation bicyclization of **12** upon organo-SOMO catalysis **17**[53] according to MacMillan's protocol generated the desired aldehyde **11** (Figures S19–S21, S42, and S43) in 72% yield with 85% enantiomeric excess (ee), which was further improved to 96% ee after a single recrystallization. The absolute configuration of **11** was unambiguously determined by X-ray crystallographic analysis (Table S44). Further three-step transformations (α-methylation to afford **18**, reduction of aldehyde, and benzylic oxidation; Figures S22–S24, S44, and S45) followed by Birch reduction and acid hydrolysis of

Please cite this article in press as: Hong et al., Photoinduced Skeletal Rearrangements Reveal Radical-Mediated Synthesis of Terpenoids, Chem (2019), https://doi.org/10.1016/j.chempr.2019.04.023

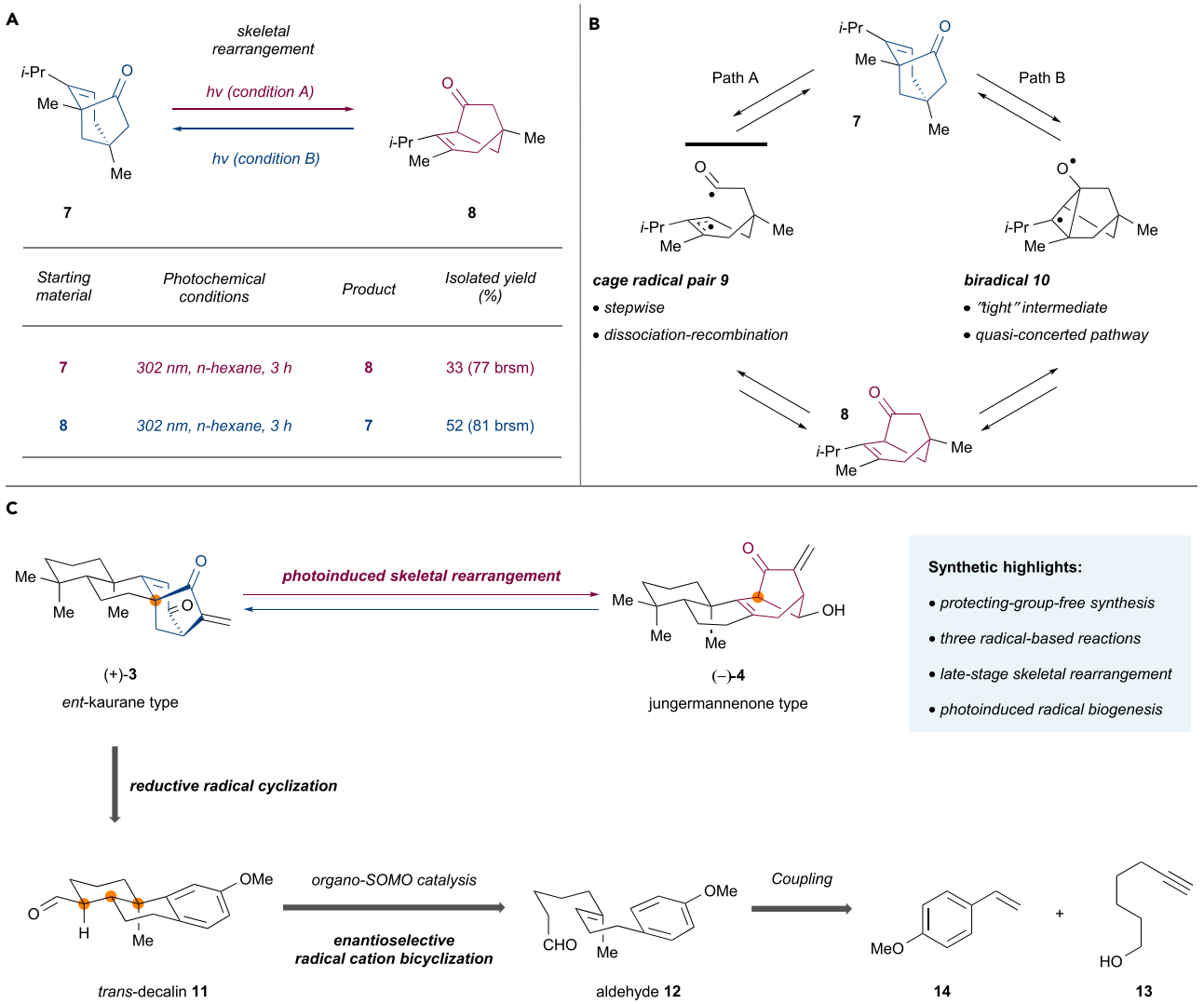

Figure 2. Photoinduced Skeletal Rearrangement of Bicyclo[3.2.1]octenes

(A) Photoinduced skeletal rearrangement of **7**, a model bicyclo[3.2.1]octene substrate.

(B) Two plausible 1,3-acyl migration mechanisms for photoinduced skeletal rearrangement.

(C) Retrosynthesis of *Isodon* diterpenoids **3** and **4**. brsm, based on recovered starting material.

the methyl enol ether *in situ* delivered dienone **19** in 41% overall yield. Stereoselective α-propargylation of **19** with **20** afforded dienyne **21**.

With dienyne **21** in hand, we sought to construct the challenging *ent*-kaurane bicyclo [3.2.1]octene framework by using 1,6-dienyne cyclization.[56] Whereas most of the catalytic cyclization conditions (cycloisomerization, reductive Heck, etc.) were found to be unsuccessful, to our delight, upon treatment of **21** with tri-*n*-butyltin hydride, dienyne reductive radical cyclization occurred exclusively at the C_8 position to give *ent*-kaurane-type scaffold **22** as the sole product (under optimized conditions), and the structure was determined by 2D NMR spectroscopy (Figures S46–S50). Interestingly, in our previous work,[56] a similar reductive radical cyclization occurred exclusively at the C_{11} position in the presence of alcohol at the C_{12} position. The present regiochemistry of radical additions to the C_8, C_9, and C_{11} positions for the *in-situ*-generated radical between **21** and the nBu_3Sn radical has been investigated by

Please cite this article in press as: Hong et al., Photoinduced Skeletal Rearrangements Reveal Radical-Mediated Synthesis of Terpenoids, Chem (2019), https://doi.org/10.1016/j.chempr.2019.04.023

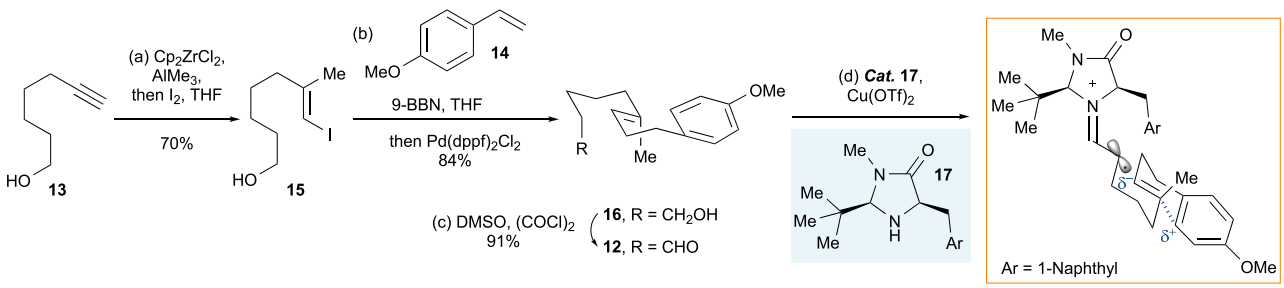

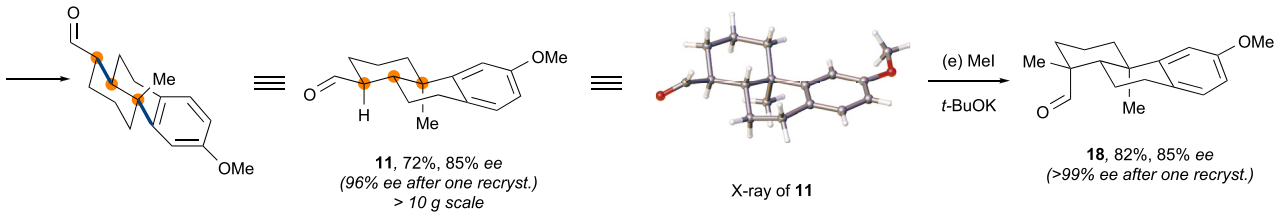

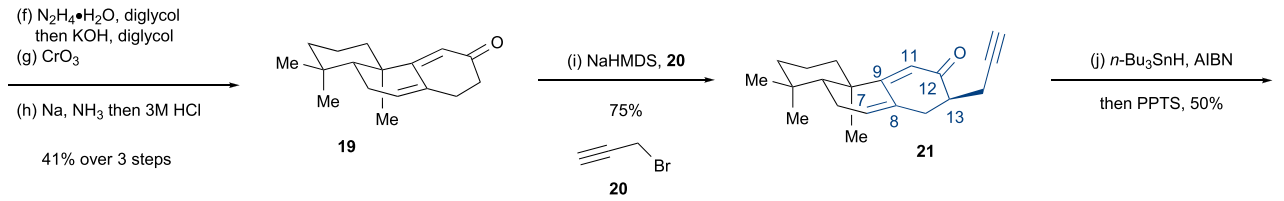

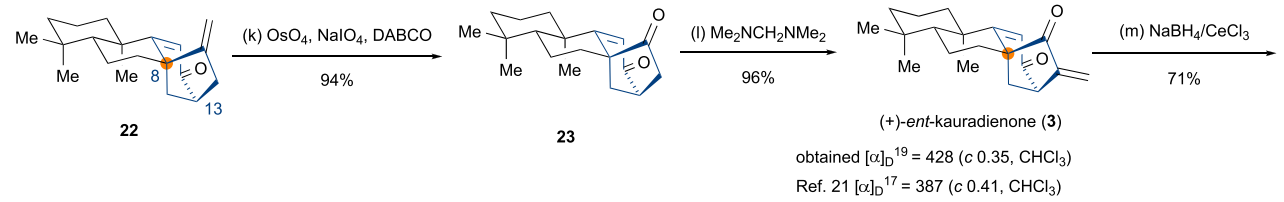

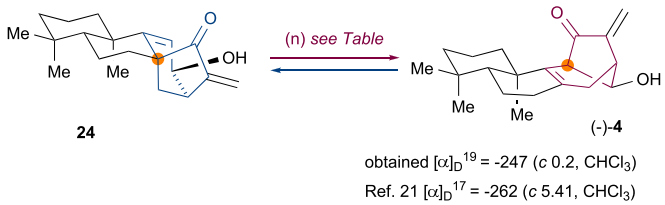

Starting material	*Photochemical conditions*	*Product*	*Isolated yield (%)*
24	***254 nm**, MeOH, rt, 3 h*	**4**	58 (81 brsm)
4	***365 nm**, n-hexane, rt, 5 h*	**24**	21 (73 brsm)
24	*sunlight, neat, 1 d*	**4**	70*
4	*sunlight, neat, 3 d*	**24**	22*

* conversion based on crude ^1H NMR

Please cite this article in press as: Hong et al., Photoinduced Skeletal Rearrangements Reveal Radical-Mediated Synthesis of Terpenoids, Chem (2019), https://doi.org/10.1016/j.chempr.2019.04.023

Figure 3. Protecting-Group-free Synthesis of *Isodon* Diterpenoids 3 and 4

Reagents and conditions are as follows: (a) Cp_2ZrCl_2, $AlMe_3$, CH_2Cl_2, −15°C, 3 h, then I_2, THF, −15°C, 2 h, 70%; (b) **14**, 9-BBN, THF, 0°C to 23°C, 5 h, then $Pd(dppf)_2Cl_2$ (10 mol%), 3M Cs_2CO_3, THF, 23°C, 10 h, 84%; (c) DMSO, $(COCl_2)_2$, Et_3N, CH_2Cl_2, −78°C to 23°C, 3.5 h, 91%; (d) **17** (30 mol %), $Cu(OTf)_2$, NaTFA, TFA, DME/MeCN (v/v = 1:1.5), 23°C, 9 h, 72%, 85% ee, 96% ee after one recrystallized from *n*-hexane; (e) MeI, *t*-BuOK, *t*-BuOH/THF (v/v = 1:2), 0°C to 23°C, 3 h, 82%, 85% ee, >99% ee after one recrystallized from *n*-hexane; (f) $N_2H_4 \cdot H_2O$, diglycol, 160°C, 2 h, then KOH, diglycol, 180°C, 6 h, 90%; (g) CrO_3, AcOH/Ac_2O (v/v = 3:1), 23°C, 7 h, 85%; (h) Na, NH_3 (liq.), EtOH, THF, −78°C, 5 h, then 3M HCl, 54%; (i) **20**, NaHMDS, HMPA, THF, −78°C, 1 h, 90%, dr 5/1; (j) *n*-Bu_3SnH, AIBN, PhMe/*t*-BuOH (v/v = 1:3), MW, 80 W, 120°C, 10 min, then PPTS, CH_2Cl_2, 23°C, 6 h, 50%; (k) OsO_4 (20 mol%), DABCO, $NaIO_4$, THF/*t*-BuOH/H_2O (v/v/v = 3:2.2:1), 23°C, 6 h, 94%; (l) $Me_2NCH_2NMe_2$, Ac_2O, DMF, MW, 80 W, 100°C, 25 min, 96%; (m) $NaBH_4$, $CeCl_3$, MeOH, −78°C, 1 h, 71%. THF, tetrahydrofuran; 9-BBN, 9-borabicyclo[3.3.1]nonane; DMSO, dimethyl sulfoxide; NaTFA, sodium trifluoroacetate; TFA, trifluoroacetic acid; DME, 1,2-dimethoxyethane; NaHMDS, sodium bis(trimethylsilyl)amide; HMPA, hexamethylphosphoramide; AIBN, azobisisobutyronitrile; MW, microwave; PPTS, pyridinium *p*-toluenesulfonate; DABCO, 1,4-diazabicyclo[2.2.2]octane; DMF, *N*,*N*-dimethylformamide; dr, diastereomeric ratio.

density functional theory (DFT) calculations,[57–59] which show that the regioselectivity is mainly controlled by geometry reason. The transition states from radical addition to both the C_9 and C_{11} positions are significantly distorted in comparison with the transition state from radical addition to the C_8 position (for more details, see Tables S24–S41 and Figures S107–112).

Upon oxidative cleavage of the *exo*-methylene moiety in **22**, diketone **23** (Figures S51 and S52) was obtained in 94% yield. Next, α-methylenation of **23** delivered (+)-*ent*-kauradienone (**3**) (Tables S6–S8; Figures S1 and S2). Selective Luche reduction of **3** furnished **24** (Figures S53–S58), which is the key proposed precursor for the photoinduced skeletal rearrangement. Upon treatment of **24** with UV irradiation at 254 nm (Table S4), (−)-jungermannenone C (**4**) (Tables S9–S11; Figures S3 and S4) was obtained in 58% isolated yield along with 28% of recovered **24**. To investigate the equilibrium nature of the photoinduced radical rearrangement, we irradiated (−)-**4** at 365 nm (Table S5). Pleasingly, **24** was generated in 21% yield along with 71% of recovered (−)-**4**. Finally, to further elucidate the biosynthetic relationship between *ent*-kaurane-type and jungermannenone-type diterpenoids, we exposed both **24** and (−)-**4** to sunlight as neat compounds. Gratifyingly, late-stage photoinduced skeletal rearrangement occurred smoothly in 22%–70% yield according to ^{1}H NMR analysis of the crude samples. Therefore, we achieved the total synthesis of (+)-*ent*-kauradienone (**3**) and (−)-jungermannenone C (**4**) in 12 and 14 steps, respectively, via late-stage photoinduced skeletal rearrangements of the bicyclo[3.2.1]octene ring system, and we thus established the absolute configurations of **3** and **4**.[21] In addition, from the interconversion between **4** and **24**, we believe that **24** is most likely a natural product.

Late-Stage Photoinduced Skeletal Rearrangements of Terpenoids

We further validated the late-stage photoinduced skeletal rearrangements by subjecting other *ent*-kaurane-type and jungermannenone-type diterpenoids or analogs to photochemical irradiation. Of note, substrates (*vide infra*) used here were either commercially available natural products or derivatives thereof (see Tables S14–S23 and Figures S7–S18). As exemplified in Figure 4, under UV irradiation, *ent*-kaurane-type diterpenoids **25** (Tables S14 and S15; Figures S7 and S8) and **26**[60] (Tables S16 and S17; Figures S9–S12) underwent photochemical rearrangement smoothly to generate, respectively, jungermannenone-type **27** (Figures S59–S64) and **28** (Figures S65–S70) and vice versa. Although we did not observe strict correlation between the UV absorption data of both *ent*-kaurane-type and jungermannenone-type products with the emission spectrum of the lamp used (Figures S103–S106), our product compositions varied drastically from different wavelengths of the lamp as well as from the different solvents used during UV irradiation. The computed energy difference of **24** and **4** (ΔG = 2.7 kcal/mol) also implies the non-existence of a thermodynamic equilibrium (Tables S42 and S43; Figure S113).

Please cite this article in press as: Hong et al., Photoinduced Skeletal Rearrangements Reveal Radical-Mediated Synthesis of Terpenoids, Chem (2019), https://doi.org/10.1016/j.chempr.2019.04.023

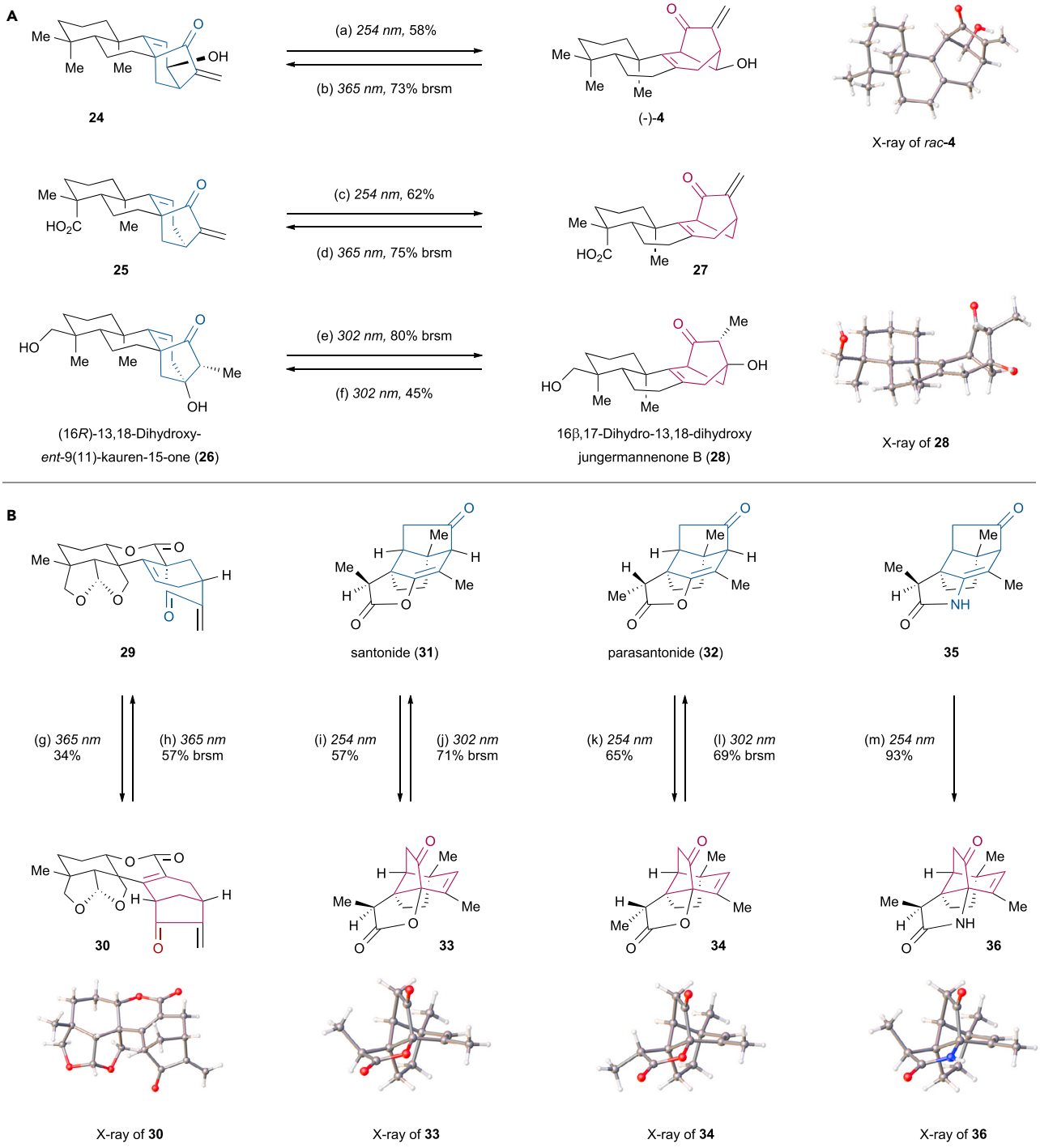

Figure 4. Late-Stage Photoinduced Skeletal Rearrangements of Terpenoids

Reagents and conditions are as follows: (a) 254 nm, MeOH, 23°C, 1.5 h, 58%; (b) 365 nm, *n*-hexane, 23°C, 5 h, 21% (73% brsm); (c) 254 nm, MeOH, 23°C, 2 h, 62%; (d) 365 nm, *n*-hexane, 23°C, 3 h, 23% (75% brsm); (e) 302 nm, MeOH, 23°C, 1 h, 27% (80% brsm); (f) 302 nm, MeOH, 23°C, 1 h, 45%; (g) 365 nm, pyridine, 23°C, 1 h, 34%; (h) 365 nm, pyridine, 23°C, 1 h, 27% (57% brsm); (i) 254 nm, *n*-hexane, 23°C, 13 h, 57%; (j) 302 nm, *n*-hexane, 23°C, 3 h, 21% (71% brsm); (k) 254 nm, *n*-hexane, 23°C, 14 h, 65%; (l) 302 nm, *n*-hexane, 23°C, 3 h, 26% (69% brsm); (m) 254 nm, MeOH, 23°C, 2 h, 93%. brsm, based on recovered starting material.

Please cite this article in press as: Hong et al., Photoinduced Skeletal Rearrangements Reveal Radical-Mediated Synthesis of Terpenoids, Chem (2019), https://doi.org/10.1016/j.chempr.2019.04.023

Collectively, and in line with the previous findings of Paquette and Meehan,[38] our results suggest that our product compositions are mostly determined by the photochemical properties of the corresponding substrates rather than their relative thermodynamic stabilities. Of note, it is also hard to correlate the optimal wavelengths with the optimal product distribution in general. As shown in Figure 4, in many cases different wavelengths were found for the interconversion after careful examination, whereas in other cases, the optimal wavelengths were identical. Next, upon UV irradiation, 6,7-seco-*ent*-kaurane-type **29** (Figures S71 and S72) also produced **30** (Figures S73–S78) in moderate yield and vice versa. Sesquiterpenoids santonide (**31**) (Tables S20 and S21; Figures S15 and S16) and parasantonide (**32**) (Tables S22 and S23; Figures S17 and S18) were then tested,[61] and to our delight, the photoinduced skeletal rearrangement of sesquiterpenoids proceeded smoothly, where the enol ether of **31** and **32** underwent photochemical rearrangement upon UV irradiation to give **33** (Figures S79–S84) and **34** (Figures S85–S90), respectively. Finally, enamide derivative **35** (Figures S91–S96) also underwent photochemical rearrangement to generate **36** (Figures S97–S102) as a sole product.

Initially, the late-stage photoinduced divergent skeletal rearrangements seemed to be unfavorable given the common belief that photolysis is too harsh and often lacks the required selectivity for complex substrates. The photoinduced transformations demonstrated here highlight the power of photochemistry for the synthesis of complex molecules,[15,16] enabling, for example, the use of well-tolerated mild reactions with unparalleled functional-group compatibility (e.g., allylic alcohols, enones, acids, free primary and tertiary alcohols, acetals, and lactones). All of the aforementioned rearranged diterpenoids were structurally determined by 2D NMR spectroscopy; among them, the structures of *rac*-**4** (Table S45), **28** (Table S46), **30** (Table S47), **33** (Table S48), **34** (Table S49), and **36** (Table S50) were confirmed by X-ray crystallographic analysis.

Conclusion

In summary, we described herein the protecting-group-free[62,63] total synthesis of two structurally diverse *Isodon* diterpenoids, **3** and **4**, in 12 and 14 steps, respectively. Our synthetic route features sequential applications of three radical-based reactions,[64–66] including the remarkable photoinduced skeletal rearrangements of bicyclo[3.2.1]octene ring systems. Further application to a series of diverse terpenoids demonstrated both the unparalleled functional-group tolerance and the broad applicability of such late-stage photochemical rearrangements for the synthesis of structurally diverse and complex small molecules. More broadly, the mild nature of late-stage photoinduced skeletal rearrangements might suggest that they are possible in a biological setting in unappreciated complimentary biosynthetic pathways,[14,67] thereby emphasizing that paying more attention to unconventional radical mechanisms could reveal exciting new chemistries in the synthesis of natural products such as terpenoids.

EXPERIMENTAL PROCEDURES

A Representative Procedure for Photoinduced Skeletal Rearrangement

Five oven-dried quartz tubes were each charged with **24** (1 mg, 3.3 μmol, 5 mg in total) and MeOH (3.3 mL, 0.001 M). The reaction mixtures were stirred while being irradiated with a 254 nm lamp at room temperature for 3 h. The reaction mixtures were combined and concentrated in *vacuo* (<25°C) and then purified by silica gel preparative TLC (petroleum ether/ethyl acetate = 4/1) to provide (−)-jungermannenone C (**4**) (2.9 mg, 58%, 81% brsm) and recover **24** (1.4 mg, 28%).

DATA AND SOFTWARE AVAILABILITY

The data for the X-ray crystallographic structures of **11**, *rac*-**4**, **28**, **30**, **33**, **34**, and **36** are available free of charge from the Cambridge Crystallographic Data Center under accession numbers CCDC: 1907703, 1875173, 1848601, 1848634, 1907653, 1848636, and 1864445, respectively.

SUPPLEMENTAL INFORMATION

Supplemental Information can be found online at https://doi.org/10.1016/j.chempr.2019.04.023.

ACKNOWLEDGMENTS

We thank Prof. Thomas J. Maimone, Prof. Ilan Marek, and Prof. Chuo Chen for helpful discussions. We thank Dr. Hiuchun Lam for language polishing and Mr. Xing Fan for assistance with computational studies. We thank Prof. Jie Su (Peking University) for assistance with X-ray analyses and crystallographic data collection and refinement and Prof. Jiang Zhou for HRMS analysis. Financial support from the NNSFC (21625201, 21661140001, 91853202, and 21521003 to X.L. and 81630093 to H.-X.L.), the National Key Research and Development Program of China (2017YFA0505200), and National High Technology Project 973 (2015CB856200) is gratefully acknowledged.

AUTHOR CONTRIBUTIONS

B.H., W.L., and J.W. contributed equally to this work. X.L., H.L., B.H., W.L., J.W., and J.W. conceived and designed the work. B.H., W.L., J. Wang, J. Wu, and Y.K. performed all the experiments. P.-J.C. and Z.-X.Y. performed all the DFT calculations. H.-X.L. provided the natural samples. H.L. and X.L. supervised the project and wrote the manuscript with assistance from B.H., W.L., J. Wang, and J. Wu.

DECLARATION OF INTERESTS

The authors declare no competing interests.

Received: December 27, 2018
Revised: March 21, 2019
Accepted: April 25, 2019
Published: May 2, 2019

REFERENCES AND NOTES

1. Clardy, J., and Walsh, C. (2004). Lessons from natural molecules. Nature *432*, 829–837.
2. Wender, P.A., and Miller, B.L. (2009). Synthesis at the molecular frontier. Nature *460*, 197–201.
3. Chen, K., and Baran, P.S. (2009). Total synthesis of eudesmane terpenes by site-selective C-H oxidations. Nature *459*, 824–828.
4. Mendoza, A., Ishihara, Y., and Baran, P.S. (2011). Scalable enantioselective total synthesis of taxanes. Nat. Chem. *4*, 21–25.
5. Jørgensen, L., McKerrall, S.J., Kuttruff, C.A., Ungeheuer, F., Felding, J., and Baran, P.S. (2013). 14-step synthesis of (+)-ingenol from (+)-3-carene. Science *341*, 878–882.
6. Kawamura, S., Chu, H., Felding, J., and Baran, P.S. (2016). Nineteen-step total synthesis of (+)-phorbol. Nature *532*, 90–93.
7. Tantillo, D.J. (2011). Biosynthesis via carbocations: theoretical studies on terpene formation. Nat. Prod. Rep. *28*, 1035–1053.
8. Gao, Y., Honzatko, R.B., and Peters, R.J. (2012). Terpenoid synthase structures: a so far incomplete view of complex catalysis. Nat. Prod. Rep. *29*, 1153–1175.
9. Christianson, D.W. (2006). Structural biology and chemistry of the terpenoid cyclases. Chem. Rev. *106*, 3412–3442.
10. Christianson, D.W. (2017). Structural and chemical biology of terpenoid cyclases. Chem. Rev. *117*, 11570–11648.
11. Yoder, R.A., and Johnston, J.N. (2005). A case study in biomimetic total synthesis: polyolefin carbocyclizations to terpenes and steroids. Chem. Rev. *105*, 4730–4756.
12. Maimone, T.J., and Baran, P.S. (2007). Modern synthetic efforts toward biologically active terpenes. Nat. Chem. Biol. *3*, 396–407.
13. Chooi, Y.-H., Hong, Y.J., Cacho, R.A., Tantillo, D.J., and Tang, Y. (2013). A cytochrome P450 serves as an unexpected terpene cyclase during fungal meroterpenoid biosynthesis. J. Am. Chem. Soc. *135*, 16805–16808.
14. Baunach, M., Franke, J., and Hertweck, C. (2015). Terpenoid biosynthesis off the beaten track: unconventional cyclases and their impact on biomimetic synthesis. Angew. Chem. Int. Ed. *54*, 2604–2626.
15. Bach, T., and Hehn, J.P. (2011). Photochemical reactions as key steps in natural product synthesis. Angew. Chem. Int. Ed. *50*, 1000–1045.

16. Kärkäs, M.D., Porco, J.A., Jr., and Stephenson, C.R.J. (2016). Photochemical approaches to complex chemotypes: applications in natural product synthesis. Chem. Rev. *116*, 9683–9747.

17. Sun, H.-D., Huang, S.-X., and Han, Q.-B. (2006). Diterpenoids from *Isodon* species and their biological activities. Nat. Prod. Rep. *23*, 673–698.

18. Liu, M., Wang, W.-G., Sun, H.-D., and Pu, J.-X. (2017). Diterpenoids from *Isodon* species: an update. Nat. Prod. Rep. *34*, 1090–1140.

19. Hong, Y.J., and Tantillo, D.J. (2010). Formation of beyerene, kaurene, trachylobane, and atiserene diterpenes by rearrangements that avoid secondary carbocations. J. Am. Chem. Soc. *132*, 5375–5386.

20. Tantillo, D.J. (2010). The carbocation continuum in terpene biosynthesis–where are the secondary cations? Chem. Soc. Rev. *39*, 2847–2854.

21. Nagashima, F., Kondoh, M., Fujii, M., Takaoka, S., Watanabe, Y., and Asakawa, Y. (2005). Novel cytotoxic kaurane-type diterpenoids from the New Zealand liverwort *Jungermannia* species. Tetrahedron *61*, 4531–4544.

22. Li, L.-M., Li, G.-Y., Xiao, W.-L., Zhou, Y., Li, S.-H., Huang, S.-X., Han, Q.-B., Ding, L.-S., Lou, L.-G., and Sun, H.-D. (2006). A new rearranged and a new *seco*-ent-kaurane diterpenoids from *Isodon parvifolius*. Tetrahedron Lett. *47*, 5187–5190.

23. Lazarski, K.E., Moritz, B.J., and Thomson, R.J. (2014). The total synthesis of *Isodon* diterpenes. Angew. Chem. Int. Ed. Engl. *53*, 10588–10599.

24. Zhu, L., Huang, S.-H., Yu, J., and Hong, R. (2015). Constructive innovation of approaching bicyclo[3.2.1]octane in *ent*-kauranoids. Tetrahedron Lett. *56*, 23–31.

25. Riehl, P.S., DePorre, Y.C., Armaly, A.M., Groso, E.J., and Schindler, C.S. (2015). New avenues for the synthesis of *ent*-kaurene diterpenoids. Tetrahedron *71*, 6629–6650.

26. Du, M., and Lei, X. (2015). Advanced in synthesis of kaurane diterpenoids. Youji Huaxue *35*, 2447–2464.

27. Toyota, M., Wada, T., Fukumoto, K., and Ihara, M. (1998). Total synthesis of (±)-methyl atis-16-en-19-oate via homoallyl-homoallyl radical rearrangement. J. Am. Chem. Soc. *120*, 4916–4925.

28. He, C., Hu, J., Wu, Y., and Ding, H. (2017). Total syntheses of highly oxidized *ent*-kaurenoids Pharicin A, Pharicinin B, 7-*O*-Acetylpseurata C, and Pseurata C: a [5+2] cascade approach. J. Am. Chem. Soc. *139*, 6098–6101.

29. Avent, A.G., Hanson, J.R., and De Oliviera, B.H. (1990). Hydrolysis of the diterpenoid glycoside, stevioside. Phytochemistry *29*, 2712–2715.

30. Hutt, O.E., Doan, T.L., and Georg, G.I. (2013). Synthesis of skeletally diverse and stereochemically complex library templates derived from isosteviol and steviol. Org. Lett. *15*, 1602–1605.

31. Cherney, E.C., Green, J.C., and Baran, P.S. (2013). Synthesis of *ent*-kaurane and beyerane diterpenoids by controlled fragmentations of overbred intermediates. Angew. Chem. Int. Ed. *52*, 9019–9022.

32. Duc, D.K.M., Fétizon, M., Hanna, I., Olesker, A., Pascard, C., and Prangé, T. (1980). An unusual acid-catalysed rearrangement of 8-methylenebicyclo[4.2.0]octan-2-ones; X-ray crystal structure of 4-isopropyl-1,5-dimethylbicyclo[3.2.1]oct-3-ene-6,7-dione. J. Chem. Soc. Chem. Commun. *24*, 1209–1210.

33. Trost, B.M., and McDougal, P.G. (1982). Total synthesis of verrucarol. J. Am. Chem. Soc. *104*, 6110–6112.

34. Ripoll, J.-L., and Vallée, Y. (1993). Synthetic applications of the retro-ene reaction. Synthesis *7*, 659–677.

35. Edmonds, D.J., Johnston, D., and Procter, D.J. (2004). Samarium(II)-iodide-mediated cyclizations in natural product synthesis. Chem. Rev. *104*, 3371–3404.

36. Nicolaou, K.C., Ellery, S.P., and Chen, J.S. (2009). Samarium diiodide mediated reactions in total synthesis. Angew. Chem. Int. Ed. Engl. *48*, 7140–7165.

37. Xia, Y., Lu, G., Liu, P., and Dong, G. (2016). Catalytic activation of carbon-carbon bonds in cyclopentanones. Nature *539*, 546–550.

38. Paquette, L.A., and Meehan, G.V. (1969). Photorearrangement of β,γ-unsaturated ketones. application to the synthesis of bridged bicyclic ketones. J. Org. Chem. *34*, 450–454.

39. Houk, K.N. (1976). The photochemistry and spectroscopy of β,γ-unsaturated carbonyl compounds. Chem. Rev. *76*, 1–74.

40. Givens, R.S., and Chae, W.K. (1978). Photorearrangements of bicyclo[3.2.l]oct-2-en-7-ones. a substituent effect study. mechanistic studies in photochemistry. 19. J. Am. Chem. Soc. *100*, 6278–6280.

41. Givens, R.S., Chae, W.K., and Matuszewski, B. (1982). Singlet-triplet reactivity of α,β,γ-unsaturated ketone: mechanistic studies in photochemistry. J. Am. Chem. Soc. *104*, 2456–2466.

42. Reimann, B., Sadler, D.E., and Schaffner, K. (1986). Gas-phase photochemistry of α,β,γ-unsaturated ketone. Concerted and radical mechanisms of the 1,3-acetyl shift in 1,2-dimethylcyclopent-2-enyl methyl ketone. J. Am. Chem. Soc. *108*, 5527–5530.

43. Wilsey, S., Bearpark, M.J., Bernardi, F., Olivucci, M., and Robb, M.A. (1996). Mechanism of the oxadi- π-methane and [1,3]-acyl sigmatropic rearrangements of β,γ-enones: a theoretical study. J. Am. Chem. Soc. *118*, 176–184.

44. Xu, G., Elkin, M., Tantillo, D.J., Newhouse, T.R., and Maimone, T.J. (2017). Traversing biosynthetic carbocation landscapes in the total synthesis of andrastin and terretonin meroterpenes. Angew. Chem. Int. Ed. *56*, 12498–12502.

45. Keylor, M.H., Matsuura, B.S., and Stephenson, C.R.J. (2015). Chemistry and biology of resveratrol-derived natural products. Chem. Rev. *115*, 8976–9027.

46. Keylor, M.H., Matsuura, B.S., Griesser, M., Chauvin, J.R., Harding, R.A., Kirillova, M.S., Zhu, X., Fischer, O.J., Pratt, D.A., and Stephenson, C.R.J. (2016). Synthesis of resveratrol tetramers via a stereoconvergent radical equilibrium. Science *354*, 1260–1265.

47. Stout, E.P., Wang, Y.-G., Romo, D., and Molinski, T.F. (2012). Pyrrole aminoimidazole alkaloid metabiosynthesis with marine sponges *Agelas conifera* and *Stylissa caribica*. Angew. Chem. Int. Ed. *51*, 4877–4881.

48. Ma, Z., Wang, X., Wang, X., Rodriguez, R.A., Moore, C.E., Gao, S., Tan, X., Ma, Y., Rheingold, A.L., Baran, P.S., and Chen, C. (2014). Asymmetric syntheses of sceptrin and massadine and evidence for biosynthetic enantiodivergence. Science *346*, 219–224.

49. Brill, Z.G., Grover, H.K., and Maimone, T.J. (2016). Enantioselective synthesis of an ophiobolin sesterterpene via a programmed radical cascade. Science *352*, 1078–1082.

50. Hung, K., Hu, X., and Maimone, T.J. (2018). Total synthesis of complex terpenoids employing radical cascade processes. Nat. Prod. Rep. *35*, 174–202.

51. Stichnoth, D., Kölle, P., Kimbrough, T.J., Riedle, E., de Vivie-Riedle, R., and Trauner, D. (2014). Photochemical formation of intricarene. Nat. Commun. *5*, 5597.

52. Roethle, P.A., and Trauner, D. (2008). The chemistry of marine furanocembranoids, pseudopteranes, gersolanes, and related natural products. Nat. Prod. Rep. *25*, 298–317.

53. Rendler, S., and Macmillan, D.W.C. (2010). Enantioselective polyene cyclization via organo-SOMO catalysis. J. Am. Chem. Soc. *132*, 5027–5029.

54. Rand, C.L., Van Horn, D.E., Moore, M.W., and Negishi, E. (1981). A versatile and selective route to difunctional trisubstituted (*E*)-alkene synthons via zirconium-catalyzed carboalumination of alkynes. J. Org. Chem. *46*, 4093–4096.

55. Chemler, S.R., Trauner, D., and Danishefsky, S.J. (2001). The *B*-alkyl Suzuki–Miyaura cross-coupling reaction: development, mechanistic study, and applications in natural product synthesis. Angew. Chem. Int. Ed. *40*, 4544–4568.

56. Liu, W., Li, H., Cai, P.-J., Wang, Z., Yu, Z.-X., and Lei, X. (2016). Scalable total synthesis of *rac*-jungermannenones B and C. Angew. Chem. Int. Ed. *55*, 3112–3116.

57. Frisch, M.J., Trucks, G.W., Schlegel, H.B., Scuseria, G.E., Robb, M.A., Cheeseman, J.R., Scalmani, G., Barone, V., Mennucci, B., Petersson, G.A., et al. (2009). Gaussian 09, Revision D.01 (Gaussian, Inc.).

58. Becke, A.D. (1993). Density-functional thermochemistry. III. The role of exact exchange. J. Chem. Phys. *98*, 5648–5652.

Please cite this article in press as: Hong et al., Photoinduced Skeletal Rearrangements Reveal Radical-Mediated Synthesis of Terpenoids, Chem (2019), https://doi.org/10.1016/j.chempr.2019.04.023

59. Lee, C., Yang, W., and Parr, R.G. (1988). Development of the Colle-Salvetti correlation-energy formula into a functional of the electron density. Phys. Rev. B Condens. Matter *37*, 785–789.

60. Lin, Z., Guo, Y., Gao, Y., Wang, S., Wang, X., Xie, Z., Niu, H., Chang, W., Liu, L., Yuan, H., and Lou, H. (2015). *ent*-Kaurane diterpenoids from Chinese liverworts and their antitumor activities through Michael addition as detected in situ by a fluorescence probe. J. Med. Chem. *58*, 3944–3956.

61. Moyano, E.L., Ceballos, N.M., Yranzo, G.I., Zinczuk, J., and Rúveda, E.A. (2005). Formation of santonide and parasantonide in the pyrolysis of santonic acid a new insight into an old reaction. ARKIVOC *xii*, 352–362.

62. Baran, P.S., Maimone, T.J., and Richter, J.M. (2007). Total synthesis of marine natural products without using protecting groups. Nature *446*, 404–408.

63. Young, I.S., and Baran, P.S. (2009). Protecting-group-free synthesis as an opportunity for invention. Nat. Chem. *1*, 193–205.

64. Jasperse, C.P., Curran, D.P., and Fevig, T.L. (1991). Radical reactions in natural product synthesis. Chem. Rev. *91*, 1237–1286.

65. Smith, J.M., Harwood, S.J., and Baran, P.S. (2018). Radical retrosynthesis. Acc. Chem. Res. *51*, 1807–1817.

66. Romero, K.J., Galliher, M.S., Pratt, D.A., and Stephenson, C.R.J. (2018). Radicals in natural product synthesis. Chem. Soc. Rev. *47*, 7851–7866.

67. The biogenesis of most *Isodon* diterpenoids is still likely to occur by carbocationic rearrangements given that these late-stage photoinduced skeletal rearrangements in general require the presence of β,γ-unsaturated ketone.